

Surface And Interface Microstructures Of Coatings Systems And Their Implication On Service Life

T Nguyen¹ X Gu¹ M VanLandingham¹ D Nguyen² M Giraud¹
¹National Institute of Standards and Technology Gaithersburg
²PPG Industries Inc Allison Park PA

Summary: The surface and interface properties have a strong influence on the adhesion and service life of polymer coatings applied to plastics and metals. However, both the surface and interface chemical composition and microstructure of coated materials are affected by the surrounding environments and processing conditions during film formation. In this study, the surface and interface properties of several coatings have been characterized with nanoscale resolution using atomic force microscopy (AFM). Specimens were prepared by applying thick films of coatings on the substrates. Both the cross-sections and surfaces that were in contact with the substrates during curing were used for the interface characterization. Interpretation of AFM results was aided by data collected using attenuated total reflection-Fourier transform infrared spectroscopy and contact angle measurements. Curing conditions and stoichiometry have a strong influence on the interface region. Further, microstructure and chemical composition of the film surface adjacent to the substrate are different from those of the surface exposed to air. The implications of these differences on the wettability, weatherability, and adhesion of coated systems are discussed.

Keywords: Interface, surface, coatings, nanoscale, AFM

1 INTRODUCTION

The surface and interface properties have a strong influence on the service life and adhesion of coatings applied to plastics and metals. However, both the surface and interface chemical composition and microstructure of coated materials are affected by the environment and processing conditions during film formation. For example, it has been established that the air surface of a multicomponent polymer system is generally enriched by a thin layer of hydrophobic material. Further, water, CO₂, and oxygen from the environment can react with certain components of a coating formulation to form side products on a coating surface. For example, water reacts readily with isocyanate in polyurethane formulations to form urea; CO₂ form salts with amine curing agents in amine-cured epoxies; and oxygen inhibits the curing of acrylic resins. Such surface enrichment and environment-induced reactions would generate a surface microstructure and chemical composition that are different from those in the bulk or at the film/substrate interface. Similarly, the buried interface/interphase between a coating and a substrate is often affected by processing conditions that control the chemical kinetics, diffusion, and volumetric changes. In addition, the interface region often includes impurities, unreacted molecules, and additives. The resulting interface/interphase is often a very complex structure, which is not easily analyzed or modeled. In this study, the interface is defined as the two-dimensional boundary between the polymer film and the substrate, while the interphase is the three-dimensional region including the interface and a zone of finite thickness on both sides of the interface. Considerable research has been conducted to improve the strength and service life of the interface/interphase region through surface treatment or modification of the substrates. However, little progress has been made in the understanding of the morphological, physical, chemical, and mechanical properties of this region, how these properties change with external stresses and processing conditions, and how this region affects the performance and service life of a polymeric system.

The main objective of this study is to characterize the surface and interface morphologies of polymer-coated materials by the use of nanoscale-resolution tapping mode atomic force microscopy. The results are presented to demonstrate that a substantial difference exists between the microstructure of the film surface exposed to air and the film surface adjacent to the substrate. These differences may have strong implications in the wettability, adhesion, and weathering resistance of coatings systems.

2 MATERIALS AND INSTRUMENTATION

2.1 Materials

Surfaces of polymer films exposed to air (air surface) and the surfaces of the same films that were in contact with the substrate during film formation (interface) were characterized using tapping mode AFM (TMAFM). In addition, the interface/interphase region of cross-sectioned samples was also studied. Samples of several different coatings having thicknesses between 50 μm and 200 μm applied to substrates were prepared by a draw-down technique. Highly-polished silicon wafers and glass plates were employed as the substrates to provide the interface samples. They were obtained by first initiating a cut through the cured coated film with a razor blade, followed by lifting up the film with a sharp knife, and peeling with a tweezers. The cross-sectioned samples were prepared from coatings applied to polished steel. Strips of coated steel were imbedded in a molding compound. Cross sections were obtained by cutting the embedded samples with a diamond saw, followed with several polishing steps; the final polish was with a 0.25 μm diamond paste.

2.2 AFM measurement

Although TMAFM is a recently-developed technique, it has become a popular tool for studying surface microstructure of polymers and biological materials because it provides a high lateral resolution with minimal damage to the samples (Magonov, 2000). In tapping mode (Fig. 1), the cantilever carrying the probing tip is oscillated at a frequency near its resonance frequency, typically, a few hundred kHz, so that the tip makes contact with the sample only for a short duration in each oscillation cycle. As the tip approaches the sample, the tip-sample interactions cause a change in the amplitude, resonance frequency, and phase angle of the oscillating cantilever. Detection of changes in the amplitude and phase shift of the cantilever probe during scanning provide topographic and phase images, respectively.

All AFM measurements were performed using a Dimension 3100 AFM (Digital Instruments)** under ambient conditions. Both AFM topographic (height) and phase images were taken. For most of the images, a set point amplitude of between 50 % and 70 % of the free amplitude was used. Silicon tips having a drive frequency of about 300 kHz and a radius of approximately 5 nm were used.

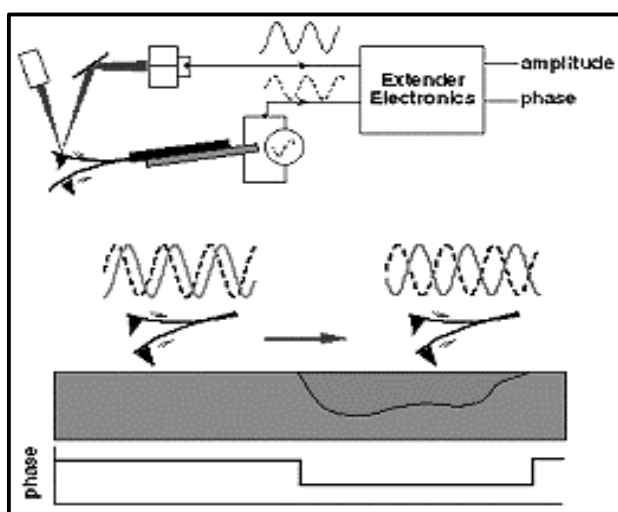


Figure 1. Tapping Mode AFM, showing cantilever oscillation amplitude and phase shift during scanning.

3 RESULTS AND DISCUSSION

3.1 AFM images of air surface and film/substrate interface

Samples of two commonly-used coatings, an amine-cured epoxy and an acrylic-melamine, applied to a very smooth silicon wafer were used to examine morphological differences between the air surface and film/substrate interface of coating systems. AFM images of the surface (a) and interface (b) for the amine-cured epoxy are displayed in Figure 2. The material was a stoichiometric mixture of a bisphenol A epichlorohydrin epoxy resin having an epoxide equivalent mass of 3050 g/mol and a polyalkoxyamine curing agent. Solutions of 50 % (by mass) epoxy resin in toluene and 50 % (by mass) amine curing agent in toluene were thoroughly mixed at appropriate ratios and applied to the Si substrates. The substrates were cleaned with acetone, followed with methanol, and dried with hot air. Coated samples were cured for 24 h at ambient condition (24 $^{\circ}\text{C}$ and 45 % RH), followed by post curing at 120 $^{\circ}\text{C}$ for 2 h. The fully-cured film had a glass transition temperature of approximately 98 $^{\circ}\text{C}$, as measured by differential scanning calorimetry. For both Figs. 2a and 2b, the pictures on the left, center, and right correspond to 3-D (dimension) topographic, 2-D topographic, and phase images, respectively. The bright and dark areas in the topographic images correspond to the surface peaks and valleys, respectively. It should be mentioned that both topographic and phase AFM

imagery taken at high magnifications showed that the silicon surface is very smooth and essentially featureless with no evidence of a surface pattern.

Figure 2 shows several morphological differences between the surface and the interface of amine-cured coatings. First, the face in contact with the substrate during film formation is considerably rougher than that of the surface exposed to air, as evidenced by the 3-D images of Fig. 2. The average roughness, root mean square (RMS), of the surface is approximately 3 nm as compared to 10 nm for the interface. It is not known whether the rough interface was actually formed during the film formation or was caused by peeling the film from the substrate.

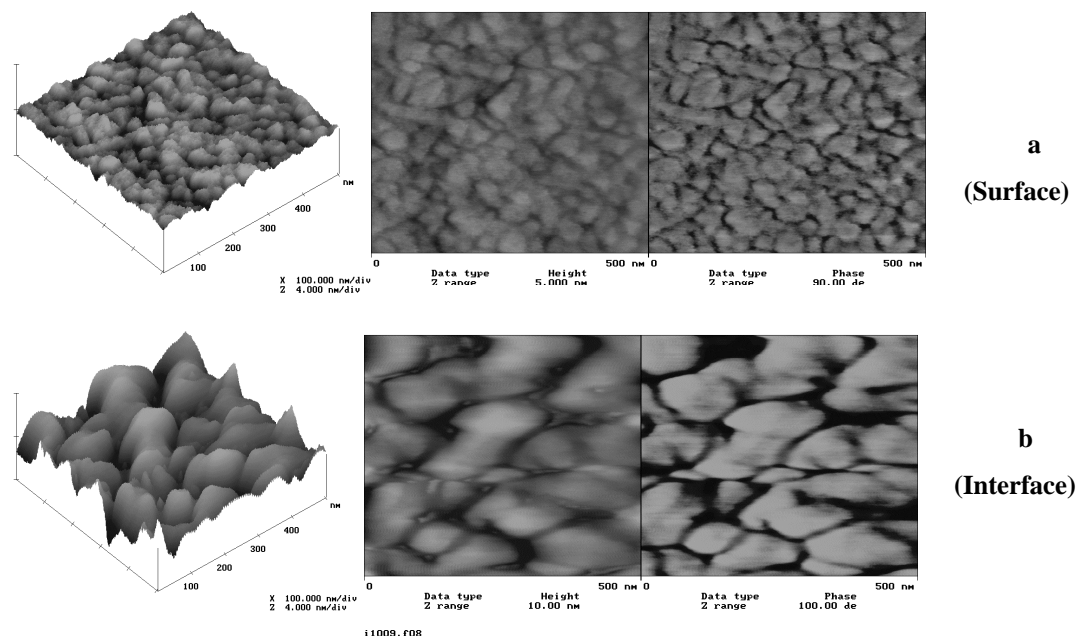


Figure 2. 500 nm x 500 nm AFM images of the surface (a) and interface (b) of a cured amine-epoxy film applied to a silicon substrate; left: 3-D topographic; center: 2-D topographic; and right: phase. Contrast variation from black to white: a) 5 nm and b) 10 nm (topographic images), a) 90° and b) 100° (phase images).

Another feature of Fig. 2 is the greater contrast and more well-defined microstructure of the interface as compared to that of the surface. Such differences between the surface and interface have been observed for other epoxies and coatings. The interface image clearly shows that the amine-cured epoxy has a two-phase microstructure, consisting of a matrix that appears bright and interstitial regions dispersed throughout the matrix that appear dark. The 500 nm regions that were imaged were very flat, with topographic changes of less than 10 nm for both the surface and interface. On the other hand, the phase angle difference between the bright and dark regions in the phase image of Fig. 2 is substantial (90° to 100°). These results indicate that the property differences between the matrix and the interstitial regions of the film are substantial.

Although the exact contrast mechanism in phase imaging is not fully understood, the bright domains in the phase image have been interpreted as due to a mechanically harder area and the dark surrounding region as due to more compliant material (Magonov et al. 1997 and Bar et al. 1997). From these assignments, the amine-cured coating shown in Fig. 2 is a heterogeneous material consisting of softer regions (dark) dispersed in a harder matrix (bright). The nodular domain in the matrix has been attributed to the high-crosslinked material and the interstitial regions as due to the less crosslinked, low molecular mass material (Cuthrell 1968, VanLandingham et al. 1999. This type of heterogeneous microstructure has been observed by AFM for other amine-cured epoxies (VanLandingham et al. 1999, Giraud et al. 2001) and polyester (Gu et al. 2001). Such inhomogeneous structure is generated during the film formation because some unreacted and partially-polymerized materials are unable to merge into the homogeneous structure and remain at the periphery of the network units [Bascom 1970]. The low crosslinked, low molecular mass region has been observed to directly correspond to the corroded spots on steel substrates (Mills and Mayne 1980). It is clear from Figure 2 that the average size of the highly-crosslinked region in the interface is larger than that on the air surface.

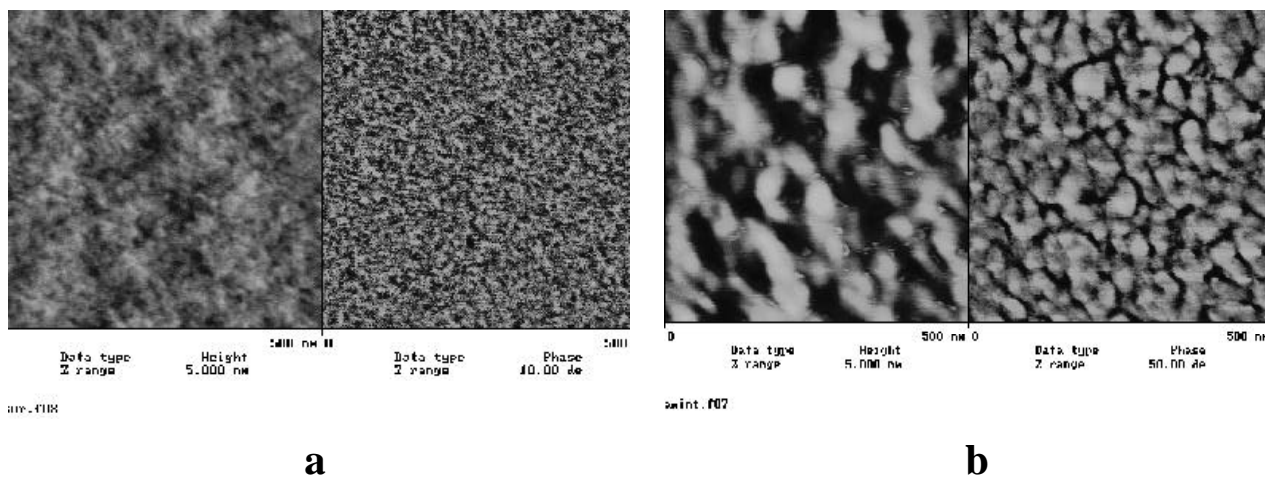


Figure 3. AFM images of the surface (a) and interface (b) of an acrylic melamine coating applied to a silicon substrate. For both a and b, topographic image is on the left and phase image is on the right.

AFM imaging of the air surface and film/substrate interface for acrylic-melamine coatings is shown in Figure 3. This material was a stoichiometric mixture of a hydroxy-terminated acrylic polymer and a partially-methylated melamine resin (Martin et al. 2001). Samples were prepared by drawing down the mixture on a cleaned, smooth silicon wafer. The cast film of approximately 50 μm thick was fully cured after heating at 130 $^{\circ}\text{C}$ for 20 minutes in an air-circulated oven. Free films were obtained by peeling from the substrate after 15-minute immersion in boiled water. The films were conditioned in a P_2O_5 -containing desiccator for one week before use. For both Figs. 3a and 3b, topographic images are on the left and phase images are on the right. As for the epoxy, the phase images show a much higher contrast and more well-defined microstructure in the interface sample than that of the surface. This difference is also indicated by a difference in the phase shift, which is only 10 $^{\circ}$ for the air side but 50 $^{\circ}$ for the substrate side. Further, even the phase image shows little evidence of the microstructure at the air surface. This observation and evidence of a well-defined microstructure at the interface, which is true for a variety of amine-cured epoxies and acrylic melamine coatings, suggests that the air surface of coatings could be covered with a thin layer of a lower surface-free-energy material. A thin layer of such a material should make the surface appear as homogeneous and with poor phase contrast, as observed in Figs. 2 and 3. This interpretation is consistent with extensive literature indicating that the air surface of a multicomponent polymer system is generally enriched with a lower surface-free-energy component to minimize polymer-air interfacial energy (Yoon et al. 1994 and Chen et al. 1998).

Since an enrichment of a hydrophobic layer at the surface has strong implications in many coating applications such as paintability, stain resistance, and weathering resistance, experiments to substantiate this postulation were conducted. Blends of low surface-free energy, crystallized poly (vinylidene fluoride) (PVDF) and amorphous poly (methylmethacrylate)-poly (ethylacrylate) copolymer (PMMA-co-PEA) are used for this study. These types of PVDF/acrylic polymer blends are commonly used for industrial coatings. Since PVDF is a crystallized polymer, it should be easily recognized when blending with amorphous materials. Fig. 4 displays 2-D and 3-D AFM topographic images of the surface and interface of the 70/30 (by mass) PVDF/PMMA-co-PEA blend. These samples were prepared by applying the blend at 47 % (by mass) in isophorone solvent to glass plates. The coated plates, which had a film thickness of approximately 75 μm , were cured at 246 $^{\circ}\text{C}$ for 10 min and cooled down slowly to 24 $^{\circ}\text{C}$. After a 10-min immersion in boiled water, the films were peeled off from the glass substrate. As seen in the 3-D images, the surface of these films is rougher than that of the interface and is covered almost

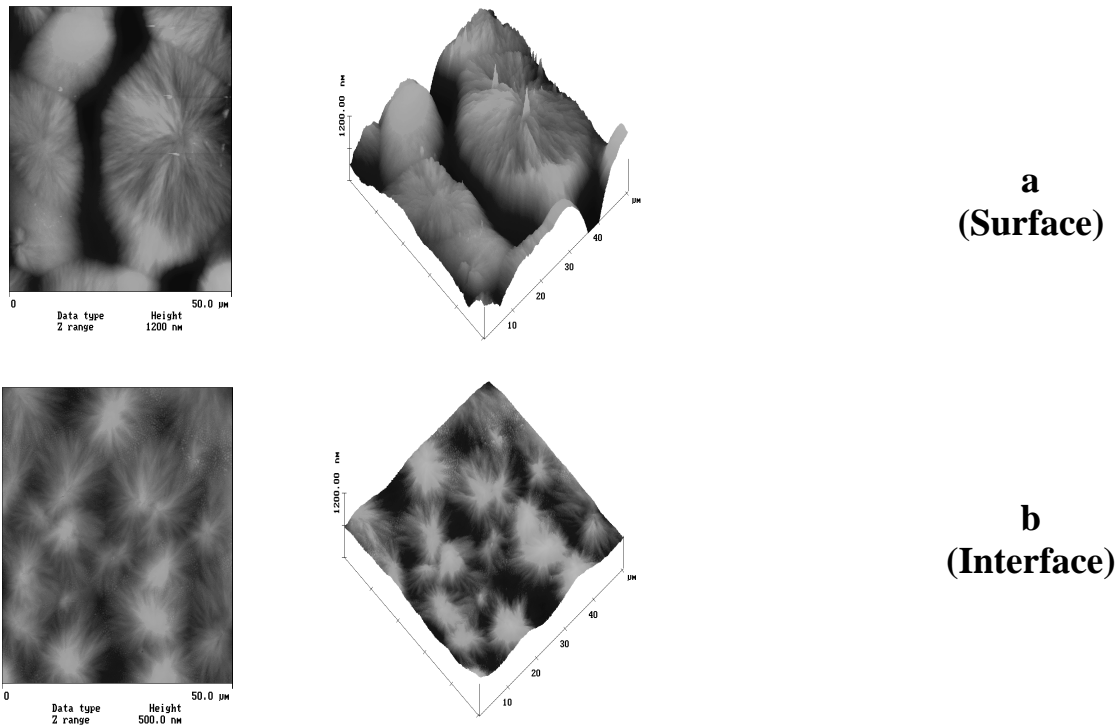


Figure 4: 50 mm x 50 mm AFM topographic images of the surface (a) and interface (b) of PVDF/PMMA-co-PEA 70/30 blend. In both a and b, 2-D image is on the left and 3-D image is on the right.

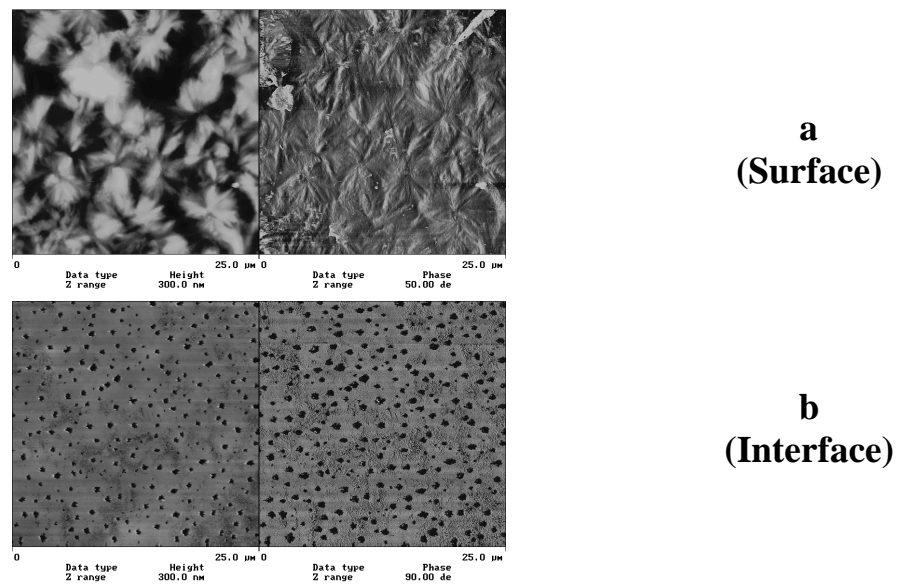


Figure 5: 25 mm x 25 mm AFM topographic and phase images of the surface (a) and interface (b) of PVDF/PMMA-co-PEA 50/50 blend. In both a and b, topographic image is on the left and phase image is on the right. Contrast variations are indicated below the images.

completely with PVDF crystallites. On the other hand, the interface is relative smooth and still contains some amorphous material. Further, the sizes of the crystal structure (spherulites) on the surface are substantially larger than those at the interface. These results indicate that the air surface of the blend films is enriched with low surface-free energy PVDF.

This is more evident in the AFM images of the 50/50 blend (by mass) shown in Fig. 5. The surface of this blend is largely covered with the crystallites of PVDF but the interface is void of crystal structure. Instead, the interface consists of smooth areas in between 200 nm to 300 nm deep holes. High magnification images of the interface revealed that the holes have an irregular shape and that these holes were actually the broken areas in the film (cohesive failure) resulting from the peeling. This observation indicates that the adhesion between the 50/50 blend and the glass substrate was good. Further, there is no evidence of the crystal structure of PVDF material at the interface even at 50 % mass fraction. Evidence provided from the

good adhesion as well as the absence of PVDF material on the film surface adjacent to the substrate suggest that amorphous PMMA-co-PEA is preferentially present at the polymer/substrate interface.

To verify that low surface-free energy PVDF preferentially migrates to the surface and higher surface-free energy acrylic copolymer tends to move to the interface, contact angle and attenuated total reflection-Fourier transform infrared spectroscopy (ATR-FTIR) analyses were performed. Contact angle is sensitive to the first 1 nm surface layer, and for the germanium prism used in this study, the ATR technique can provide chemical information at a depth from about 0.25 μm to 1.0 μm from the surface for wavelengths of infrared radiation from 3 μm to 10 μm . Therefore, these analyses should provide information on the chemical composition at or near the surface. The results are summarized in Table 1.

Table 1. Surface and interface wettability and ATR-FTIR properties of different PVDF/PMMA-co-PEA blends

PVDF/PMMA-co-PEA blends, mass fraction

	70/30		50/50		30/70	
	Surface	Interface	Surface	Interface	Surface	Interface
Water Contact Angle, degrees ¹	71.5 \pm 0.9 ²	58.3 \pm 0.5	72.5 \pm 3.7	68.1 \pm 4.7	75.1 \pm 1.4	63.5 \pm 1.9
Surface Polarity	0.21	0.5	0.17	0.46	0.16	0.29
C-F/C=O ³	0.382	0.331	1.02	0.92	2.25	2.06

¹Average of six measurements; ²The number after the \pm symbol indicates one standard uncertainty; ³FTIR-ATR intensity ratio between the C-F band and C=O band.

In Table 1, the contact angle was measured using the sessile drop method, and the results were the average of six drops. The surface polarity is the ratio between the polar force component and the total surface free energy. These surface parameters were determined using the geometric mean method (Wu 1982) and with water and methylene iodide as the liquids. Both the contact angle and surface-free energy components, namely polar force and nonpolar force, can give a good indication of the wetting and related properties of a surface. The C-F/C=O is the ratio between the ATR-FTIR intensity of the C-F band of PVDF material and C=O band of the acrylic copolymer. All results of Table 1 show that the surface contains a larger amount of the less wettable, low surface-free energy PVDF than the interface. This observation supports the AFM results given above.

The results presented in Figs. 2 to 5, and Table 1 clearly show that a substantial difference exists in the microstructure between the surface and interface and that a low surface-free energy layer is present on the film surface exposed to air. Since the microstructure and chemical composition of a surface control its interactions with other materials and the environments, such a low surface-free energy surface should have a large effect on the wettability and weatherability of coatings. For example, the paintability and bondability to such a surface is more difficult than to more hydrophilic surfaces. On the other hand, it is a harder surface for dirt and contaminants to stick to and an easier surface for slipping (low friction). A low surface-free energy covered surface would also alter the weather resistance of the coatings. This is because, while the bulk coating underneath degrades, the more inert, hydrophobic thin layer on the surface may not undergo any change at all until much later times. This was the case for the degradation of acrylic-melamine coatings exposed to humid environments (Nguyen et al. 2001). In this study, FTIR analyses indicated substantial hydrolysis and material loss in the film within a few 200 h of exposure. However, AFM results showed little surface morphology and roughness change until after 600 h exposure. Similarly, the delay in the hydrolysis of poly(sebacic anhydride) (PSA) and poly(DL-lactic acid) (PLA) blends used to control drug deliveries has been verified by AFM and X-ray photoelectron spectroscopy (XPS) as due to a surface enrichment of the more hydrolytically-resistant PLA (Chen et al. 1998). The difference in the degradation characteristics between the surface and the bulk could explain the lack of a correlation between surface gloss loss and bulk chemical degradation, often reported in the coatings literature.

3.2 AFM images of coating system cross sections

Another approach to investigate the difference between surface and the interface is to compare AFM images of the air surface with those of the cross sections. Examples for a two-part polyurethane (PU) and an amine-cured epoxy coating are illustrated in Figs. 6 and 7, respectively. These are 3-D AFM topographic images of cross sections of thick films applied to a polished steel surface. Figure 6a shows a cross-sectioned image of a PU sample cured at ambient (24 $^{\circ}\text{C}$ and 45 %RH) for two weeks, and Figure 6b is from the same PU sample but cured at 100 $^{\circ}\text{C}$ in an air-circulated oven for 2 h. The interface region (interphase) is defined as the rough section between the steel and the smooth PU matrix. The large difference between the peaks and valleys in the interphase was apparently induced by the mechanically weak material of this region and was roughened by the polishing action. These results suggest that the roughened section of these samples was not fully cured. This is supported by the smoothness of the PU matrix further away from the substrate. Such a smooth appearance indicates a more fully-cured and hard surface. It is not certain whether the weak interphase was due to an inadequate curing schedule (short time or low

temperature) or due to a consumption of isocyanate by the hydrated steel surface. A post-curing study at an elevated temperature for different times could provide an answer to this question. Nevertheless, a sample containing such a weak interface region will have poor adhesion. Figure 6 also shows that the weak interface region of the heat-cured sample was narrower than that of the ambient-cured sample. These results suggest that AFM can be an useful technique to study the effect of curing schedule on the adhesion and service life of coating systems and adhesives.

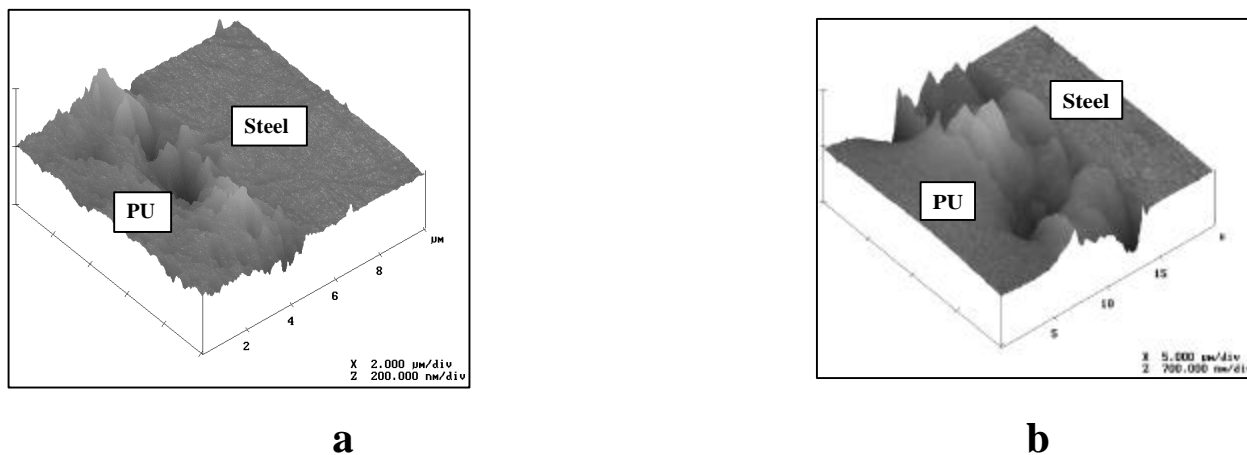


Figure 6. AFM 3-D topographic images of room-temperature cure (a) and heat-cure (b) polyurethane coating on steel.

Figure 7 shows the effect of epoxy/amine ratio on the interface region of an amine-cured epoxy coating. The epoxy resin was a 190 g/m equivalent mass material and the amine was a polyalkoxyamine. All samples were cured at 120 °C for 2 h. In the excess-amine sample (Figure 7c), the polished epoxy surface is smoother than that of the 1/1 and 1/0.8 epoxide/amine samples. Further, the rough, undercured interface region of the excess-amine sample ($\approx 1.8 \mu\text{m}$) is narrower than that of the 1/1 amine/epoxide sample ($\approx 4 \mu\text{m}$). On the other hand, the amine-deficient sample (Figure 7a) shows no distinctive interface region. The rough nature of this cross section, which is similar to the interface regions of the other two stoichiometric samples, suggests that the amine-deficient sample was not fully cured. A difference in the interphase width between the 1/1 and 1/1.2 epoxide/amine samples suggest that the interphase under-cure region was wider for the 1/1 epoxy/amine sample than that of the excess-amine epoxy. This postulation is consistent with previous reports indicating that amines from amine-cured epoxies have a tendency to migrate and preferentially adsorb on glass fiber (Palmese and McCullough 1992) and hydrated steel (Wicks 1987) surfaces. It is noted that, under ambient condition, a layer of iron oxides approximately 35 nm to 40 nm is instantaneously formed on the steel surface. Since iron oxides are highly energetic, they adsorb water rapidly. Thus, it is expected that the surface of the polished steel used in this study was covered with a hydrated oxide layer. The migration of amine to the substrate surface not only leaves the material near the interface under-cured, which results in weak adhesion, but also produces an interface with an excess of amine. Since low molecular mass amines are hygroscopic, the presence of such material at the interface will introduce an osmotic pressure when this material is exposed to water or high relative humidities. This will result in an increase in the rate of water transport to the interface and an increase of the thickness of the water layer at that location. Thus, if the substrate is not properly treated or the coating is not properly formulated, the interface of amine-cured coated materials in humid environments is susceptible to water attack, resulting in loss of adhesion and delamination.

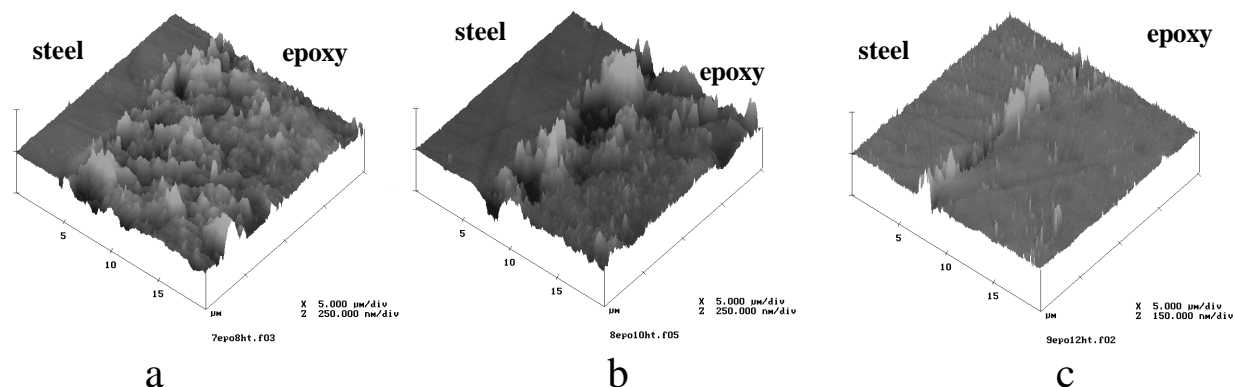


Figure 7. 15 mm x 15 mm AFM 3-D topographic images of amine-cured epoxy coated steel having different epoxide/amine ratios; a) epoxide/amine: 1/0.8; b) epoxide/amine: 1/1; and c) epoxide/amine:1/1.2.

4 CONCLUSIONS

The surface and interface microstructure of a variety of coatings applied to different substrates have been characterized with nanoscale resolution by tapping mode atomic force microscopy (TMAFM). Contact angle measurements and attenuated total reflection-Fourier transform infrared spectroscopy were performed on some coating systems to verify AFM data. In addition, the effects of curing conditions and stoichiometry on the interface region were also studied for polyurethane and epoxy coatings. The results show that the surface exposed to the substrate has a much higher contrast and a more well-defined morphology than those of the surface exposed to air. This result suggests that there is a substantial difference in both chemical composition and microstructure between the surface and interface, and that a thin layer of a low surface-free energy material generally covers coating surface. These results have strong implications for many phenomena occurring on the surface of coating systems, including the wettability, bondability, paintability, and weatherability.

***Certain commercial product or equipment is described to specify adequately the experimental procedure. In no case does such identification imply recommendation or endorsement by NIST, nor does it imply that it is necessarily the best available for the purpose.*

5 REFERENCES

1. Bascom, W.D. 1970, 'Water at the interface', *J. Adhesion*, 2, 161-183.
2. Bar, G., Thomann, Y., Brandsch, R. & Whamgho, M.H. 1997, 'Factors affecting the height and phase images in tapping mode atomic force microscopy. Study of phase-separated polymer blends of poly(ethene-co-styrene) and poly(2,6-dimethyl-1,4-phenylene oxide)', *Langmuir*, 13, 3807-3812.
3. Chen, X., McGurk, S.L., Davies, M.C., Roberts, C.J., Shakesheff, K.M., Tendler, S.J.B. & Williams, P.M. 1998, 'Chemical and morphological analysis of surface enrichment in a biodegradable polymer blend by phase-detection imaging atomic force microscopy', *Macromolecules*, 31, 2278-2283, and references therein.
4. Cuthrell, R.E. 1968, 'Epoxy polymers. II. Macrostructure', *J. Appl. Polym. Sci.*, 12, 1263-1278.
5. Giraud, M., Nguyen, T., Gu, X. & VanLandingham, M.R. 2001, 'Effects of stoichiometry and epoxy molecular mass on wettability and interfacial microstructures of amine-cured epoxies', Proc. 24th Annual Meeting of the Adhesion Society, ed J.A. Emerson, pp 260-261.
6. Gu, X., Raghavan, D, Nguyen, T, & VanLandingham, M.R. 2001, 'Characterization of polyester degradation in alkaline solution with AFM tapping mode: Exposure to NaOH at room temperature', *Polym. Deg. and Stab*, in press.
7. Magonov, S.N., Elings, V. & Whangbo, M.H. 1997, 'Phase imaging and stiffness in tapping mode atomic force microscopy', *Surf. Sci.*, 375, L385-L391.
8. Magonov, S.N. 2000, 'Atomic force microscopy in analysis of polymers', in *Encyclopedia of Analytical Chemistry*, ed R.A. Meyers, John Wiley and Sons, Chichester, pp. 7432-7491.
9. Mills, D.J. & Mayne, J.E.O. 1981, 'The inhomogeneous nature of polymer films and its effects on resistance inhibition, in *Corrosion Control by Organic Coatings*, ed H. Leihseier, Jr., Nat. Assoc. Corr. Eng., Houston, TX, pp.12-17.
10. Nguyen, T., Gu, X., VanLandingham, M.R., Giraud, M., Dutruc-Rosset, R, Ryntz, R. & Nguyen, D. 2001, 'Characterization of coatings interphase with phase imaging AFM, Proc. 24th Annual Meeting of the Adhesion Society, ed J.A. Emerson, pp 68-69.
11. Nguyen, T., Martin, J., Saunders, S. & Byrd, E. 2001, 'Modes, mechanism and model for the hydrolysis of acrylic-melamine coatings in the absence of UV light', Submitted to *Journal of Coatings Technology*.
12. Palmese, G.R & McCullough, R.L. 1992, 'Effect of epoxy amine stoichiometry on cured resin material properties', *J. Appl. Polym. Sci.*, 46, 1863-1873.
13. VanLandingham, M.R., Eduljee, R.F. & Gillespie, J.W., Jr. 1999, 'Relationships between stoichiometry, microstructure, and properties for amine-cured epoxies', *J. Appl. Polym. Sci.*, 71, 699-711.
14. Wu, S. 1982. *Polymer Interface and Adhesion*, Marcel Dekker, Inc. N.Y., p.181.
15. Wicks, Z.W. 1987, '*Corrosion Protection by Coatings*', Federation Series on Coatings Technology, Federation of Societies for Coatings Technology, Philadelphia, PA, pp 7-22.
16. Yoon, S.C., Ratner, B.D., Ivanc, B. & Kennedy, J.P. 1994, 'Surface and bulk structure of segmented poly(ether urethanes) with perfluoro chain extenders. 5. Incorporation of poly(dimethylsiloxane) and polyisobutylene macroglycols', *Macromolecules*, 27, 1548-1554